SUPPORTING INFORMATION

Nanoplatelet size to control the alignment and thermal conductivity in copper-graphite composites

André Boden, Benji Boerner, Patryk Kusch, Izabela Firkowska and Stephanie Reich

Department of Physics, Freie Universität Berlin, Arnimallee 14, 14195 Berlin, Germany

S1 Sample Characterization

The graphite nanoplatelets with various lateral sizes were purchased from commercial sources (Tab IS). As presented in Fig. 1S (left panel), both, the GnP M5 and M25 flakes have rigid form, whereas T80 shows wavy-like appearance, which might be related to its big lateral size.

TABLE IS Characteristics of graphite nanoplatelet

Material abbreviation	Commercial source	Lateral size (μm)	Thickness (nm)
M5	XG Sciences, Inc.	5	20
M25	XG Sciences, Inc.	25	20
T80	TIMCAL Inc. C-Therm	80	50

The microstructure of the composites was investigated on the fractured surface; this was achieved by breaking the "coin"- composite (the ruptures occurred at the middle regions of the tested samples).

Figure 1S (right panel) reviles relatively rough surface of the ruptured samples and orientation of the graphite nanoplatelets, which is in particular visible for composite with M25 and T80 fillers. In addition, no agglomeration of the GnP could be visible upon high resolution SEM investigation.

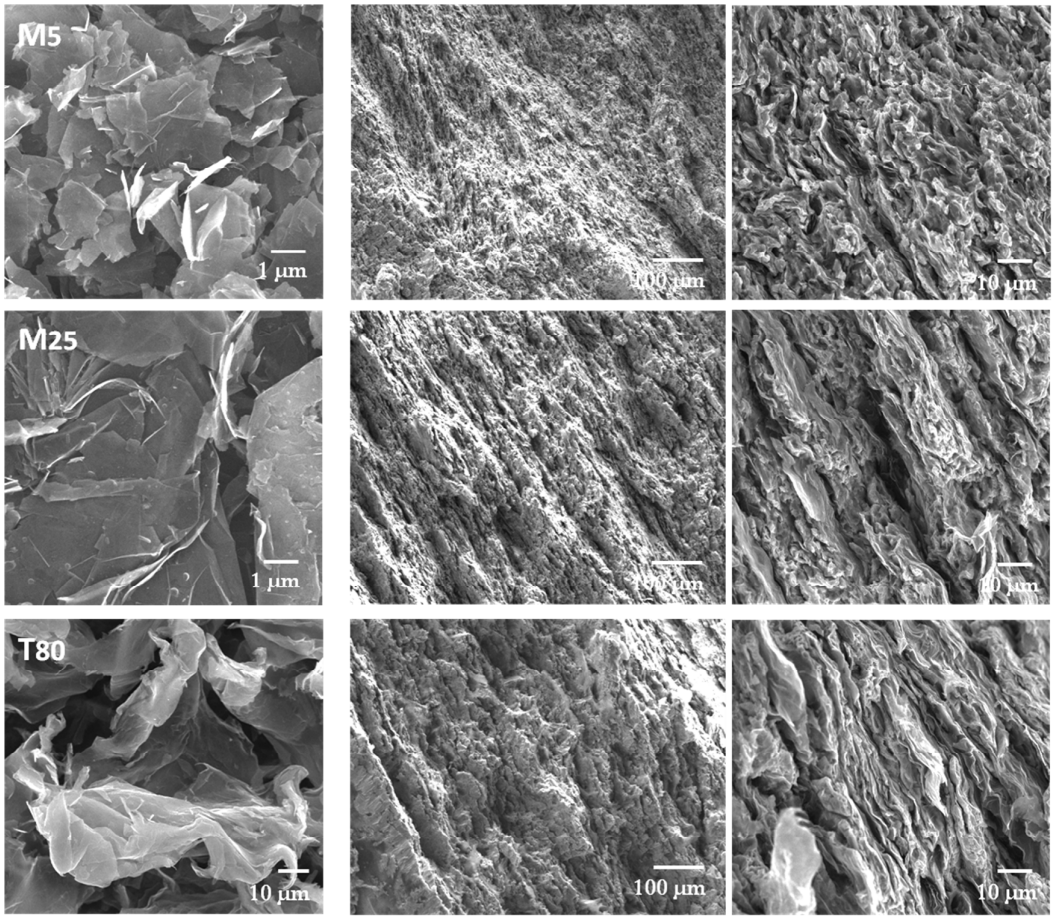

Figure 1S: SEM images of nanoscale fillers (left panel) and fractured surfaces of sintered Cu-GnP composites (middle panel) depicting orientation direction of the fillers within the copper (right panel).

The influence of the ball milling as well as sintering on the disorder of the GnPs was investigated using Raman spectroscopy on as received GnPs as well as the copper-GnP powder mixture after ball milling and sintering. Representative Raman spectra are shown in Fig. 2S for T80 GnPs. Comparing the D-peak intensities before and after ball milling one can see a slight increase of the D-peak intensity after ball milling. The D/G-intensity ratio increases from 0.16 to 0.31 indicating an increased disorder introduced to the GnPs. However, this increase is not significant. Furthermore, spark plasma sintering does not increase the disorder of the GnPs within the copper matrix as the D/G-intensity ratio remains constant at 0.31.

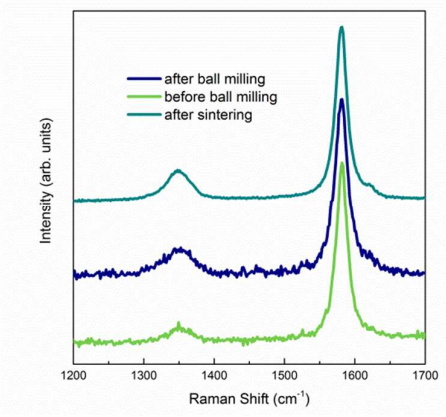

Figure 2S: Representative Raman spectra of T80 GnPs before and after ball milling

The measurements of thermal diffusivity were carried out on NanoFlash Netzsch LFA 447 that uses a 0.06 – 0.31 ms Xenon lamp pulse to heat the sample one side. The resulting temperature rise on the other side of the sample is recorded using an infrared detector. Both the in-plane and through-plane diffusivity were measured on the same sample. Moreover, the in-plane diffusivity measurements were realized using special sample holder (Fig. 3S). Prior the diffusivity measurements each sample was coated with a few micrometer-thick layer of graphite.

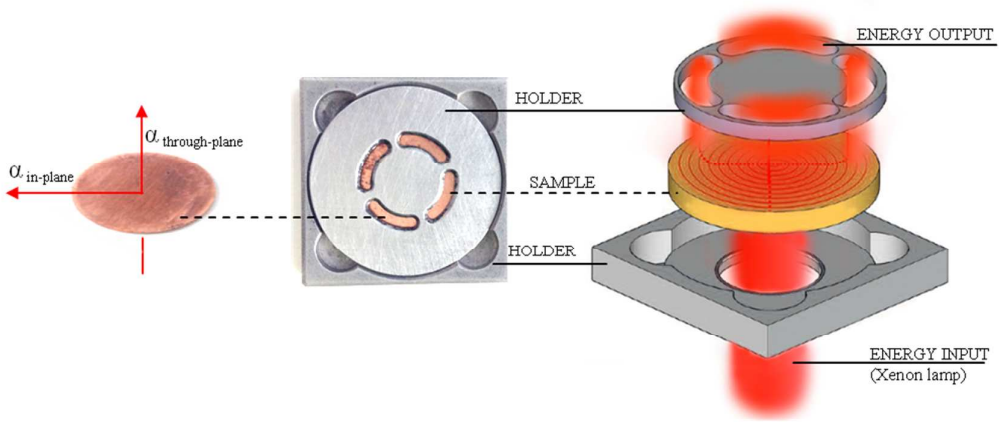

Figure 3S: Sample and the schematic of the xenon flash measurement with a special sample holder, which allows determining thermal diffusivity in the in-plane direction.

S2 Polarized Raman Theory

The intensity of the Raman active modes can be calculated using the selection rules for light scattering in crystals described elsewhere[1]. With that one can predict the intensity of the E_{2g} mode (G-Peak) of graphite in dependence of the light polarization as well as the orientation of the graphite basal plane. To calculate the G mode intensity as a function of internal GnP alignment and external polarization direction we transform the Raman tensor of the E_{2g} phonon from the frame of an individual GnP into the lab frame. For a single graphite nanoplatelet with a certain orientation in the matrix the G-peak intensity can then be calculated using[1,2]

$$I_{GnP}(\gamma_1,\gamma_2) \propto \langle e_{in}\ \Gamma_x^{\dagger}(\gamma_1)\Gamma_y^{\dagger}(\gamma_2)\boldsymbol{R_1}\Gamma_x(\gamma_1)\Gamma_y(\gamma_2)\ e_{sc}\rangle^2 + \langle e_{in}\ \Gamma_x^{\dagger}(\gamma_1)\Gamma_y^{\dagger}(\gamma_2)\boldsymbol{R_2}\Gamma_x(\gamma_1)\Gamma_y(\gamma_2)\ e_{sc}\rangle^2, \quad (1)$$

with

$$e_{in} = e_{sc} = \begin{pmatrix}\cos(\varepsilon)\\ 0\\ \sin(\varepsilon)\end{pmatrix};\ \boldsymbol{R_1} = \begin{pmatrix}0 & f & 0\\ f & 0 & 0\\ 0 & 0 & 0\end{pmatrix};\ \boldsymbol{R_2} = \begin{pmatrix}f & 0 & 0\\ 0 & -f & 0\\ 0 & 0 & 0\end{pmatrix};$$

$$\Gamma_x(\gamma) = \begin{pmatrix}1 & 0 & 0\\ 0 & \cos(\gamma) & -\sin(\gamma)\\ 0 & \sin(\gamma) & \cos(\gamma)\end{pmatrix};\ \Gamma_y(\gamma) = \begin{pmatrix}\cos(\gamma) & 0 & \sin(\gamma)\\ 0 & 1 & 0\\ -\sin(\gamma) & 0 & \cos(\gamma)\end{pmatrix};$$

where e_{in} and e_{sc} are the polarization vectors of the incoming and scattered light, $\boldsymbol{R_1}$ and $\boldsymbol{R_2}$ are the Raman tensors of the E_{2g} mode and $\Gamma_{x,y}(\gamma_{1,2})$ are rotation matrices which rotate the Raman tensors about the x- and y-axis by the angle γ_1 and γ_2. To obtain the overall intensity we now integrate over all possible GnP orientations

$$I_{tot} \propto \iint g(\gamma_1,\sigma)\, g(\gamma_2,\sigma)\, I_{GnP}(\gamma_1,\gamma_2)\, d\gamma_1 d\gamma_2, \quad (2)$$

with

$$g(\gamma,\sigma) = \frac{1}{\sigma\sqrt{2\pi}}\exp\left(-\frac{\gamma^2}{2\sigma^2}\right),$$

where $g(\gamma_{1,2})$ is the angle distribution for the rotation angles γ_1 and γ_2. For a random distribution of the GnPs (i.e. $g(\gamma_{1,2}) = 1$) one expects a constant intensity of the G-peak when varying the polarization angle ε. For perfectly aligned GnPs (i.e. $\gamma_1 = \gamma_2 = 0$) the intensity $I_{tot} \propto f^2 \cos^4\varepsilon$ and thus has a maximum

for the in-plane polarization ($\varepsilon = 0, \pi,$ and 2π); it is zero for $\varepsilon = \pi/2, 3\pi/2$. Both cases are shown in Fig. 5S(a). If we assume a normal distribution of the angles γ_1 and γ_2 one can find a standard deviation σ for all possible intensity dependences between random and full alignment. As a reference we measured highly-oriented pyrolytic graphite (HOPG) were the graphite layers are fully aligned (Fig. 4S).

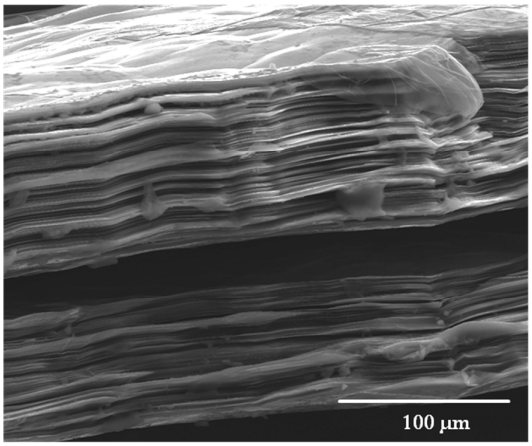

Figure 4S: SEM image of a layered structure of HOPG.

As presented in Fig. 5S(b) one can see that the Raman intensity of the G-peak is not zero for polarization perpendicular to the layers. This is a result of the rough surface of the fractured cross section as well as introduced disorders of the graphite planes at the point of the fracture due to breaking the material. Furthermore, the finite collection angle of the laser using a NA = 0.25 objective leads to non-zero intensity for $\varepsilon = \pi/2, 3\pi/2$. To take this into account we modify Eq. (2) by introducing the additional intensity contribution I_0 which leads to the corrected intensity for HOPG

$$I_{tot} \propto \iint g(\gamma_1, \sigma)\, g(\gamma_2, \sigma)\, I_{GnP}(\gamma_1, \gamma_2)\, d\gamma_1 d\gamma_2 + I_0. \quad (3)$$

From HOPG we obtain I_0, thus, the standard deviation σ remains the only free parameter to match the Raman intensity for the three composite types. Using Eq. (3) we find $\sigma = 0.67$ for M5, 0.58 for M25, and 0.46 for T80 composites to fit the experimental Raman intensities presented in Fig. 5S.

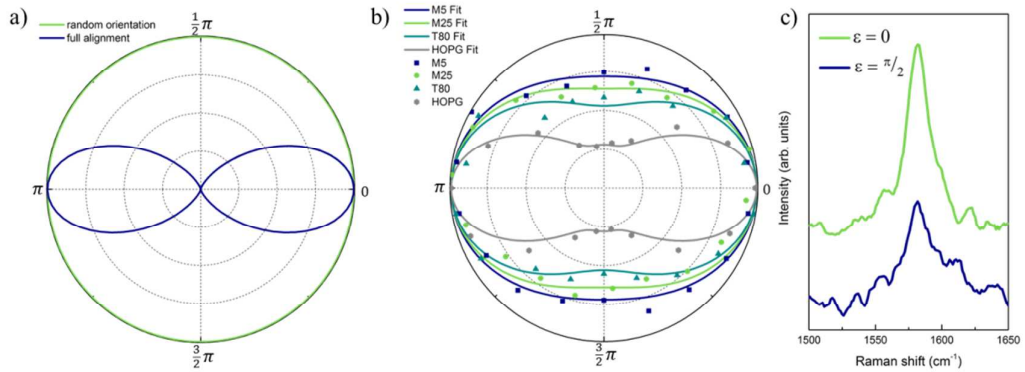

Figure 5S: (a) G-mode intensity for randomly oriented and fully aligned GnPs (b) G-mode intensity for M5, M25 and T80 composites and HOPG as a function of the angle ε between the polarization of the incoming light and the composite in-plane axis. The measured data (symbols) are fitted to Eq. 3 (solid lines) and (c) Raman spectra of the G-mode for T80 composite with parallel and perpendicular polarization.

S3 EMA Modulation for Thermal Conductivity Enhancement Calculations

To derive the thermal conductivity of the described composite materials we use the model developed by Nan *et al.*[3] within the effective medium approximation. It describes the effect of geometry, concentration, thermal conductivity, and orientation of the filling material as well as the thermal interface resistance between matrix and filler on the TCE of the composite. The thermal conductivity of the composite with respect to its symmetry axes is given by[3]

$$k_{11} = k_{22} = k_m \frac{2+f[\beta_{11}(1-L_{11})\,(1+\langle cos^2\theta\rangle)+\beta_{33}(1-L_{33})\,(1-\langle cos^2\theta\rangle)]}{2-f[\beta_{11}\,L_{11}\,(1+\langle cos^2\theta\rangle)+\beta_{33}\,L_{33}\,(1-\langle cos^2\theta\rangle)]} \quad (4)$$

and

$$k_{33} = k_m \frac{1+f[\beta_{11}(1-L_{11})\,(1-\langle cos^2\theta\rangle)+\beta_{33}(1-L_{33})\,\langle cos^2\theta\rangle]}{1-f[\beta_{11}\,L_{11}\,(1-\langle cos^2\theta\rangle)+\beta_{33}\,L_{33}\,\langle cos^2\theta\rangle]}. \quad (5)$$

with

$$\beta_{ii} = \frac{k_{fii}-k_m}{k_m+L_{ii}(k_{fii}-k_m)}, \quad (6)$$

$$L_{11} = L_{22} = \frac{p^2}{2\,(p^2-1)} + \frac{p}{2\,(1-p^2)^{3/2}}\, cos^{-1}p, \quad (7)$$

and

$$L_{33} = 1 - 2\,L_{11}. \quad (8)$$

Here $k_{11} = k_{22}$ and k_{33} are the effective thermal conductivities of the composite in the in-plane and through-plane direction, respectively, f is the volume fraction of the GnP particles, k_m is the thermal conductivity of the matrix, and p (= thickness / length) is the aspect ratio of the GnP. k_{fii} is given by[3]

$$k_{fii} = \frac{k_{GnPii}}{1+(1+2\,p)\,k_{GnPii}\,L_{ii}\,R_k/d}, \tag{9}$$

where k_{GnPii} is the intrinsic thermal conductivity of the GnP in corresponding direction, d is the thickness of the GnP, and R_k is the thermal interface resistance between matrix and GnP (Kapitza resistance). The statistical orientation of the GnP particles is represented by $\langle cos^2\theta \rangle$ which equals 1/3 for totally randomly oriented GnP particles and becomes one for fully aligned fillers. It is given by[3]

$$\langle cos^2\theta \rangle = \frac{\int \varphi(\theta)\, cos^2\theta\, sin\theta\, d\theta}{\int \varphi(\theta)\, sin\theta\, d\theta}, \tag{10}$$

With

$$\varphi(\theta) = \frac{1}{\sigma\sqrt{2\pi}} \exp\left(-\frac{\theta^2}{2\sigma^2}\right)$$

where θ is the angle between the symmetry axes of the composite and the GnP particles and $\varphi(\theta)$ describes the statistical distribution of θ using σ as determined by Raman measurements. For T80 composites $\langle cos^2\theta \rangle$ was found to be 0.69 leading to a Kapitza resistance of $R_k = 1.0 \cdot 10^{-9}$ m^2KW^{-1}. To point out the huge influence of GnP alignment we compare the obtained TCE results to a composite will fully aligned T80 GnPs. As shown in Fig. 6S (a) the in-plane thermal conductivity is expected to increase to up to 600 $Wm^{-1}K^{-1}$ for concentrations of 25 vol%. Furthermore, assuming an interface resistance one order of magnitude higher than the obtained one the resulting thermal conductivity is found to be below 150 $Wm^{-1}K^{-1}$ for concentrations of 25 vol% as presented in Fig. 6S(b).

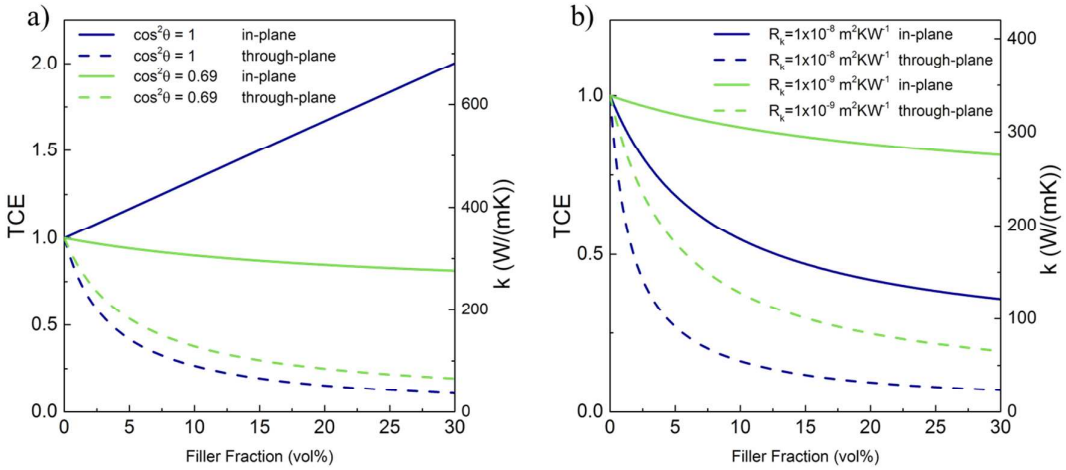

Figure 6S: (a) TCE of T80 composites for the obtained GnP orientation in comparison with T80 composites with fully aligned GnPs and (b) TCE of T80 composites with obtained Kapitza resistance in comparison with 10 times higher Kapitza resistance.

5

References

10 (1) Cardona, M. In *Light Scattering in Solids II*; Cardona, P. D. M.; Güntherodt, P. D. G., Eds.; Topics in Applied Physics; Springer Berlin Heidelberg, 1982; pp. 19–178.

(2) Reich, S.; Thomsen, C. *Philos. Trans. R. Soc. Lond. Ser. Math. Phys. Eng. Sci.* **2004**, *362*, 2271–2288.

(3) Nan, C.-W.; Birringer, R.; Clarke, D. R.; Gleiter, H. *J. Appl. Phys.* **1997**, *81*, 6692.

15